energy&fuels

pubs.acs.org/EF

Article

Empirical Kinetic Models for the Combustion of Charcoals and Biomasses in the Kinetic Regime

Gábor Várhegyi,* Liang Wang, and Øyvind Skreiberg

Cite This: https://dx.doi.org/10.1021/acs.energyfuels.0c03248

Read Online

ACCESS | Metrics & More | Article Recommendations | Supporting Information

ABSTRACT: An empirical kinetic model was proposed in 2019 and tested extensively on biomass pyrolysis (Várhegyi, G., *Energy Fuels* **2019**, *33*, 2348−2358). The model was based on an isoconversional kinetic equation. The functions in the kinetic equation were approximated by mathematical formulas with adjustable parameters, and the parameters were determined by the method of least squares. This procedure ensures that the data calculated from the model would be close to the experimental data. In the present work, this way of modeling was adapted for the combustion of charcoals and lignocellulosic biomasses. The performance of the model was tested by the reevaluation of TGA experiments from earlier publications. In total, 18 experiments belonged to a study of charcoals, while 20 experiments were carried out on wheat straw and willow samples. The corresponding temperature programs included linear, modulated, stepwise, and constant reaction rate (CRR) temperature−time functions. The adjustable parameters of the model were determined by the method of least squares by evaluating groups of experiments together. The procedure aimed at finding best-fitting models for the derivative of the measured reacted fraction. The activation energy, E, was regarded as constant for the whole process. The change of the reactivity during the progress of the reaction was described by the rest of the isoconversional kinetic equation. Model variants with different numbers of adjustable parameters resulted in practically identical E values. It was possible to determine common E values for different samples with only a slight worsening of the fit quality. This procedure allowed an easy comparison of the reactivities of the samples as functions of the reacted fraction.

1. INTRODUCTION

The combustion of the various biomasses and chars of biomass origin is an important part of the renewable energy production. Thermogravimetric analysis (TGA) is a useful method to study the kinetics of the corresponding processes in the kinetic regime due to its high precision.[1] However, particular care is needed to avoid the overheating or the self-ignition of the samples during the experiments because of the huge reaction heat of the combustion.[2] In the case of ideal chars (i.e., specially prepared pure model carbons), the reaction rate is proportional to the surface area, and the change of the surface area during the reaction can be described by theoretical models.[3−5] In the case of real chars, however, complicating factors arise. One of them is inhomogeneity: typical charcoal contains parts with different reactivities, which can be described by more than one kinetic equation. The combustion of lignocellulosic materials is a particularly complex process because it involves thermal decomposition of several organic compounds and the decomposition is followed by the burn-off of the formed chars. The studies based on more than one kinetic equation usually employ a least-squares evaluation, which allows the determination of the model parameters and ensures the fit between the experimental data and the data calculated from the model.[6−18] Another branch of the studies is based on much simpler isoconversional methods.[19−26] In these works, the activation energy, E, and the pre-exponential factor, A, are regarded as functions of the reacted fraction, α, and the combustion is described by an equation of type

$$\frac{d\alpha}{dt} = A(\alpha)f(\alpha)\exp\left(-\frac{E(\alpha)}{RT}\right) \quad (1)$$

where $A(\alpha)$, $f(\alpha)$, and $E(\alpha)$ are empirical functions. Obviously, only the product of $A(\alpha)$ and $f(\alpha)$ can be determined from the experimental data. More precisely, an empirical $[A(\alpha)f(\alpha)]$ function can be factored to $A(\alpha)$ and $f(\alpha)$ parts in an infinite number of ways. For historical reasons, the kinetic evaluations by eq 1 are frequently called "model-free" methods. This term is misleading because eq 1 itself is a model.[27] It is more precise to call eq 1 "isoconversional", which means that the reaction rate, $d\alpha/dt$, is a function of the temperature at any selected α value and does not depend on the temperature history that led to a given (α, T) point.[27] The fit between the experimental data and the data calculated from the kinetic model usually is not checked in the works employing isoconversional kinetics.[28] The isoconversional evaluations frequently result in too high or too low E values. For example, Várhegyi quoted E values between 10 and 1327 kJ/mol from the literature of biomass pyrolysis.[28] The works cited in the present work also contain unrealistic E values. For instance, the work by Lotfi et al. shows E versus α graphs where E ranges from 5 to 31 kJ/mol for

Received: September 27, 2020
Revised: November 6, 2020

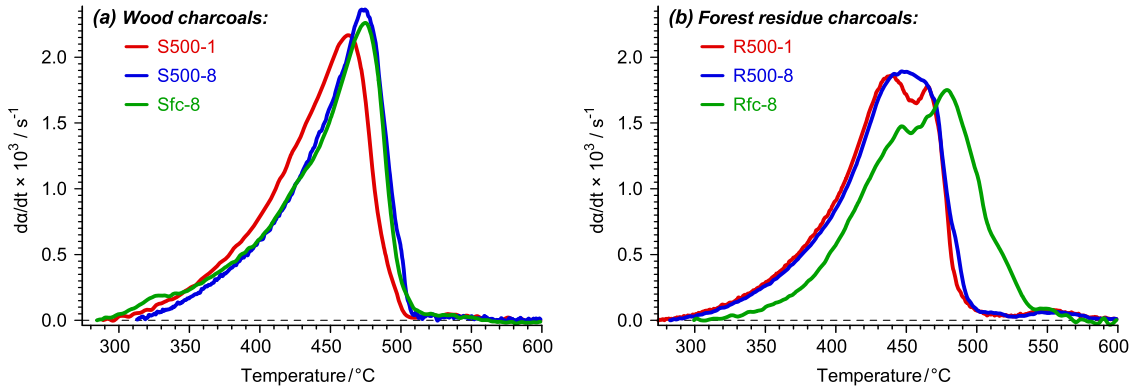

Figure 1. Comparison of the combustion of the charcoal samples at 10°C/min heating. (a) Charcoals prepared from spruce wood and (b) charcoals prepared from forest residue. (See more details about the samples and their combustion in the paper of Wang et al.[16])

pyrolysis and from ca. 5 to ca. 90 kJ/mol for oxidative thermolysis.[23] In our opinion, however, even an empirical E should correspond to the IUPAC definition of the activation energy: "an empirical parameter characterizing the exponential temperature dependence of the rate coefficient".[29] In this respect, the too low and too high E values do not reflect the usual temperature dependences of the reaction rates in the kinetic regime.[28]

Várhegyi proposed best-fitting models based on eq 1 with a limited number of adjustable parameters, which can be determined by the method of least squares.[28] The method is based on the application of simple polynomial functions. In this way, practical empirical models can be obtained, which describe the reactions at different temperature programs. The method was tested on the pyrolysis of 16 biomass samples including woody biomass, agricultural residues, and industrial waste. Altogether 85 TGA experiments were evaluated in these tests. Their temperature programs comprised constant heating rates, stepwise heating, constant reaction rate heating, isothermal temperature programs, and a modulated temperature program.[28] It turned out that constant activation energies with variable $[A(\alpha)f(\alpha)]$ functions can also provide reasonable fit qualities for the biomass pyrolysis.[28] The corresponding results were reinforced in subsequent work as well.[30] At constant E, eq 1 is simplified to

$$\frac{da}{dt} = A(a)f(a)\exp\left(-\frac{E}{RT}\right) \tag{2}$$

where the variation of the reactivity during the pyrolysis is described by the $[A(\alpha)f(\alpha)]$ function. It was approximated by a simple empirical function with six adjustable parameters, while the E value was an additional parameter to be determined by the method of least squares.[28,30] The use of eq 2 has some advantages: No unrealistic E values appeared in this way. Besides, the change of the reactivity with α can be surveyed easily. Finally, the calculation by the kinetic model is much faster when a huge number of evaluations are needed at a given set of model parameters. Hence, a two- or three-dimensional numerical modeling can be carried out more easily with such models. The variables can be separated in eq 2 as follows

$$\int_0^\alpha \frac{d\alpha}{A(\alpha)f(\alpha)} = \int_0^t \exp\left(-\frac{E}{RT}\right)dt \tag{3}$$

where the left-hand side is denoted by $g(\alpha)$. One can easily calculate thousands of values for $g(\alpha)$ at a given set of parameters by numerical integration before the start of compute-intensive modeling. The $g(\alpha)$ values can be stored together with the corresponding α and $[A(\alpha)f(\alpha)]$ values in an array. At each right-hand-side value arising during the modeling, the software can search for the nearest $g(\alpha)$ in the array by a fast binary search algorithm, and the corresponding α and $[A(\alpha)f(\alpha)]$ values are immediately available for the calculations.

The preceding two works on this method were based only on pyrolysis processes.[28,30] In the present work, the applicability of eq 2 is extended to the combustion of charcoals and biomasses, and the properties of the obtained models are surveyed.

2. SAMPLES AND METHODS

2.1. Samples and Experiments. Such TGA experiments are reevaluated in the present work that had been evaluated earlier by other models.

(i) In total, 18 TGA experiments on six charcoal samples were reevaluated from the work of Wang et al.[16]

(ii) In total, 20 TGA experiments on the wheat straw and willow wood samples were reused from the work of Várhegyi et al.[12]

Particularly low sample masses were employed in all TGA experiments. Their actual values depended on the heating program as well as on the reactivity of the sample. Figure 1 in the work of Wang et al.[16] shows that an initial sample mass of 0.6 mg results in the self-ignition of the char sample at 10 °C/min, while a smaller sample of 0.2 mg results in a regular, kinetically controlled TGA curve. In the case of biomass samples, a heating rate of 40 °C/min required an initial sample mass of 0.3 mg, while it was possible to employ 1.5 at a much slower heating rate of 4 °C/min. The Supporting Information of the present work indicates the initial sample mass for each reevaluated experiment.

2.2. Model. Herewith we briefly summarize the methods proposed in 2019 for the parametrization of eq 2.[28] A kinetic equation must obviously provide $d\alpha/dt = 0$ when the reaction species are consumed, i.e., when $\alpha = 1$. A simple rearrangement of eq 2 helps to fulfill this condition easily

$$\frac{d\alpha}{dt} = \tilde{A}(\alpha)(1-\alpha)\exp\left(-\frac{E}{RT}\right) \tag{4}$$

where $\tilde{A}(\alpha)$ is $A(\alpha)f(\alpha)/(1-\alpha)$ when $\alpha < 1$. The division by $(1-\alpha)$ is not possible at the $\alpha = 1$ point, but $\tilde{A}(\alpha)$ can have any finite positive value there. This rearrangement facilitates further work. By taking the logarithm of $\tilde{A}(\alpha)$ and rearranging eq 4, we get

$$\frac{d\alpha}{dt} = (1-\alpha)\exp\left(\ln\tilde{A}(\alpha) - \frac{E}{RT}\right) \tag{5}$$

https://dx.doi.org/10.1021/acs.energyfuels.0c03248
Energy Fuels XXXX, XXX, XXX−XXX

Function $\ln \tilde{A}(\alpha)$ can be approximated by simple polynomials. In our previous works, $\ln \tilde{A}(\alpha)$ was approximated by fifth-order polynomials[28,30]

$$\ln \tilde{A}(\alpha) = b_0 + b_1\alpha + b_2\alpha^2 + b_3\alpha^3 + b_4\alpha^4 + b_5\alpha^5 \quad (6)$$

In the present work, we employed higher-order polynomials as well because

(i) The inhomogeneities in charcoal may result in irregular shapes in the experimental $d\alpha/dt$ curves.
(ii) The combustion of lignocellulosic material results in two peaks on the $d\alpha/dt$ curves: one for the pyrolysis and another for the burn-off of the formed chars.

We shall turn back to these points in the treatment.

The approximations with high-order polynomials cannot be carried out without a suitable parameter transformation, which decreases the interdependence of the variables. Chebyshev polynomials of the first kind were employed for this purpose because their calculation is simple and fast through their well-known recurrence relations. Accordingly, the α variable was transformed to the $[-1, +1]$ interval

$$x = 2\alpha - 1 \quad (7)$$

and eq 6 was replaced by

$$\ln \tilde{A}(x) = c_0 + c_1T_1(x) + c_2T_2(x) + c_3T_3(x) + \ldots + c_nT_n(x) \quad (8)$$

where n is the order of the polynomial, $c_0 \ldots c_n$ are coefficients to be determined by the method of least squares, and the values of $T_1(x) \ldots T_n(x)$ are calculated by the recurrence relations of the Chebyshev polynomials of the first kind. The Supporting Information of the present work contains a brief example code both in C and Fortran languages for the easy calculation of the right-hand side of eq 8 at any α and n values.

2.3. Evaluation by the Method of Least Squares and Characterization of the Fit Quality. Such values were searched for the unknown model parameters, which minimize the difference between the experimental $(d\alpha/dt)^{obs}$ and the predicted $(d\alpha/dt)^{calc}$ data. The experimental reacted fractions were calculated as

$$\alpha^{obs}(t) \cong \frac{m_0^{obs} - m^{obs}(t)}{m_0^{obs} - m_{600\,°C}^{obs}} \quad (9)$$

where $m^{obs}(t)$ is the sample mass at time t and m_0^{obs} is the sample mass at the start of the reaction. In the biomass combustion of the present work, m_0^{obs} was selected to be the sample mass at 120 °C. Here, the drying of the sample has terminated already while the oxidative pyrolysis has not started yet. The situation was less simple in the char combustion experiments because the combustion was preceded by a mass gain due to oxygen chemisorption. As an approximation, the start of the mass-losing part of the curve was selected for m_0^{obs}, as shown in the char combustion figures later in the text and in the Supporting Information. The end point of the reaction could be set to around 600 °C in all cases.

The experimental $d\alpha/dt$ values were obtained by approximating the $\alpha^{obs}(t)$ values by smoothing splines.[31] The root-mean-square difference between the original $m(t)$ and the smoothing spline was typically much below 1 μg. Such small differences do not introduce considerable systematic errors into the least-squares kinetic evaluations.[32]

The method of least squares is carried out by finding the model parameters, which minimize the following objective function

$$of = \sum_{j=1}^{N_{exper}} \sum_{i=1}^{N_j} \frac{\left[\left(\frac{d\alpha}{dt}\right)_j^{obs}(t_i) - \left(\frac{d\alpha}{dt}\right)_j^{calc}(t_i)\right]^2}{N_j h_j^2} \quad (10)$$

where N_{exper} is the number of experiments evaluated together, N_j is the number of t_i time values in experiment j, and h_j is the highest experimental point on the given experimental curve. The division by h_j^2 serves for normalization.

The obtained fit quality can be characterized separately for each of the experiments evaluated together. For this purpose, the relative deviation (reldev, %) is used. The root-mean-square (rms) difference between the observed and calculated values is expressed as a percent of peak maximum.

$$\text{reldev}(\%) = 100\left\{\sum_{i=1}^{N_j} \frac{\left[\left(\frac{d\alpha}{dt}\right)_j^{obs}(t_i) - \left(\frac{d\alpha}{dt}\right)_j^{calc}(t_i)\right]^2}{N_j h_j^2}\right\}^{0.5} \quad (11)$$

The fit quality for a given group of experiments is characterized by the root mean square of the corresponding relative deviations. For example, the root-mean-square reldev for 18 experiments is denoted by reldev_{18}.

The least-squares evaluations were carried out by simple but safe numerical methods. The experimental temperature values were connected by linear interpolation and eq 1 was solved by a Runge–Kutta method for each experiment in each (t_{i-1}, t_i) interval.[33] The minimization of the objective function was carried out by a variant of the Hook–Jeeves method. The Hook–Jeeves method is a slow but simple and dependable direct search algorithm.[34] Further details can be found about the employed numerical methods in the earlier works of Várhegyi et al.[9,12,28] The present work is based on hundreds of least-squares evaluations by eq 10. So many calculations obviously needed some automation, as described earlier.[28]

3. CHARCOAL COMBUSTION

3.1. About the Experiments Reevaluated. Charcoals were prepared from spruce wood and from forest residues by three different methods resulting in six charcoal samples. Letters S and R in the names of the samples stand for spruce and forest residue, while substrings "500−1" and "500−8" denote preparations in a macro-TGA at 1 and 8 bar pressures. A third preparation method, identified by substring "fc-8", employed a flash carbonization process.[16] TGA experiments with linear, modulated, and constant reaction rate (CRR) experiments were employed for each charcoal.[16] Figure 1 compares the behavior of the samples at 10 °C/min heating.

The present evaluation of these TGA experiments was carried out by two evaluation approaches as follows.

3.2. Approach I: Each Sample is Evaluated Separately. The three TGA experiments for a given sample were evaluated separately from the other samples by the method of least squares. Various degrees of polynomials, n, were employed. The results are shown in Table 1. The second column is the degree of polynomial in the given evaluations. It is followed by the root-mean-square fit quality calculated for all of the 18 experiments, reldev_{18}. One E value was obtained for each sample in this way, hence six E values were obtained for the six charcoals. Table 1 lists their average, E_{aver}, and their extrema, E_{lowest} and $E_{highest}$. These values do not depend significantly on n. Note that a scatter of 1 kJ/mol is negligible.[35] The reldev_{18} and E values listed in Table 1 suggest that all of the tested polynomial orders resulted in suitable models for the studied char samples. We selected $n = 9$ for the illustration of the results because the fit improves till $n = 9$ for both evaluation strategies. The best, worst, and typical fits are shown by red lines in Figure 2.

3.3. Approach II: Models with Identical Activation Energy for all Samples. This approximate modeling helps to survey and compare the reactivities of the samples, as outlined in the next section. Technically a grid of E values was selected in the middle part of the domain obtained in approach I: 149,

https://dx.doi.org/10.1021/acs.energyfuels.0c03248
Energy Fuels XXXX, XXX, XXX−XXX

Table 1. Evaluations of the Char Samples with Different Degrees of Polynomials[a,b]

approach	n	reldev$_{18}$	$E_{average}$	E_{lowest}	$E_{highest}$
I	5	4.2	151	137	166
I	6	4.2	151	137	166
I	7	4.0	152	138	166
I	8	3.8	152	138	166
I	9	3.7	152	138	167
I	10	3.7	152	138	166
I	11	3.7	152	138	167
I	12	3.7	152	138	167
I	13	3.6	152	138	167
II	5	4.8	150		
II	7	4.7	150		
II	9	4.4	150		
II	11	4.4	150		
II	13	4.4	150		

[a]In total, 18 experiments on six charcoal samples were evaluated by two approaches employing different degrees of polynomials, n, in the model. reldev$_{18}$ is the root-mean-square relative deviation calculated for 18 experiments. The lowest and highest E values are not listed for the evaluations by approach II because the E values were identical for the six charcoals in those cases. [b]The dimensions of E and reldev$_{18}$ are kJ/mol and %. See the text for further details.

150, 151, 152, and 153 kJ/mol. All least-squares evaluations were carried out with these E values at n = 5, 7, 9, and 13. The lowest reldev$_{18}$ values were found at E = 150 kJ/mol at each n. The reldev$_{18}$ values obtained so are shown in the lower part of Table 1. One can see that reldev$_{18}$ is decreasing till n = 9, as mentioned above. The $(d\alpha/dt)^{calc}$ curves obtained at E = 150 kJ/mol and n = 9 are shown in blue color in Figure 2 for the experiments presented there. (Note that the "best", "worst" and "typical" adjectives in the legends of Figure 2 refer to the curves obtained by approach I.) All the 18 $(d\alpha/dt)^{calc}$ curves belonging to E = 150 kJ/mol and n = 9 are shown in the Supporting Information.

3.4. Comparing the Reactivity of the Samples. The reactivity of a sample is usually expressed as $(d\alpha/dt)/(1-\alpha)$. For the char + oxygen reactions, this concept was introduced by Radović et al.[36] The term "specific reactivity" is also used for the same expression.[37] Using the notation of the present work, we get the following from eq 4 at $\alpha < 1$

$$\frac{d\alpha/dt}{1-\alpha} = \tilde{A}(\alpha)\exp\left(-\frac{E}{RT}\right) \quad (12)$$

Approach II results in models with identical E for all samples, hence the reaction differences between the samples are connected to their $\tilde{A}(\alpha)$ functions. Figure 3 shows $\log_{10}\tilde{A}(\alpha)$ for each sample. It is interesting to observe the sudden drop of reactivity around $\alpha \approx 1$ in Figure 3b. This behavior is nearly identical for the three forest residue chars. There is a side peak in the $(d\alpha/dt)^{obs}$ curves after the main part of the burn-off of the forest residue chars, as shown by the corresponding figures in the Supporting Information. Wang et al.[16] attributed this side peak to the thermal decomposition of inorganic carbonates in the ash of the forest residue chars. The drop around $\alpha \approx 1$ in Figure 3b expresses the low reactivity

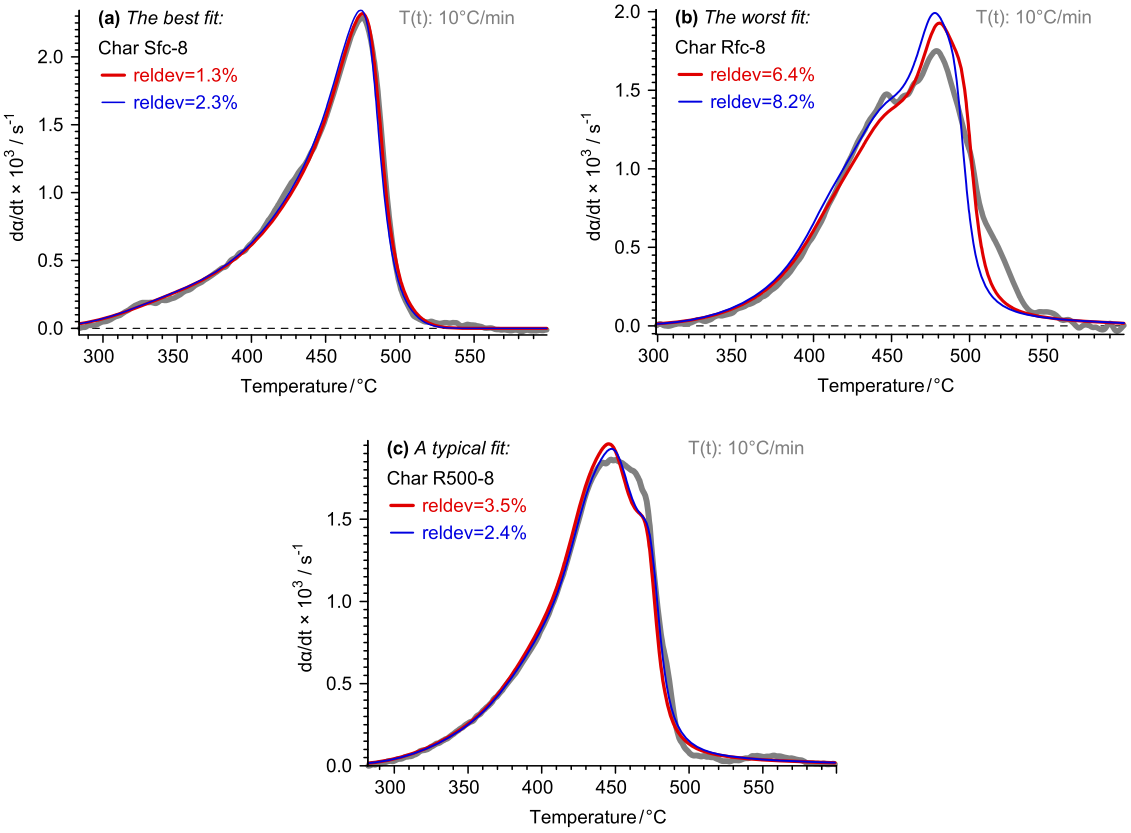

Figure 2. Illustration of the best (a), worst (b), and typical (c) fit qualities obtained for the charcoal samples by approach I at n = 9. The corresponding $(d\alpha/dt)^{calc}$ curves are denoted by red color. The $(d\alpha/dt)^{calc}$ curves determined by approach II for the same experiments at E = 150 kJ/mol are also indicated. They are shown by thin blue lines. The thick gray lines represent the $(d\alpha/dt)^{obs}$ curves.

https://dx.doi.org/10.1021/acs.energyfuels.0c03248
Energy Fuels XXXX, XXX, XXX−XXX

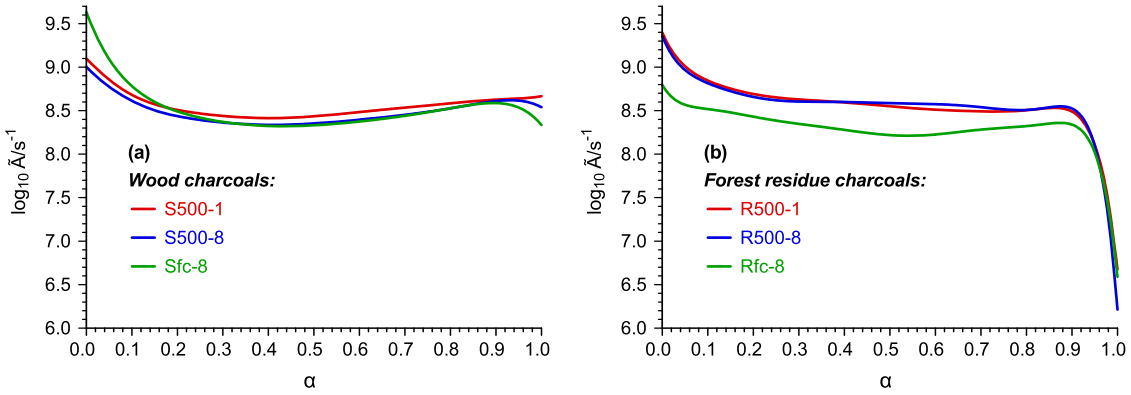

Figure 3. The functions of $\log_{10} \tilde{A}(\alpha)$ for the six charcoal samples at E = 150 kJ/mol and n = 9. (a) Charcoals prepared from spruce wood and (b) charcoals prepared from a forest residue.

(slow thermal decomposition) of the carbonates between 500 and 600 °C. The data shown in Figure 3 provide a clearer view on the reactivity differences than the direct comparison of the experiments shown in Figure 1. For example, the $\log_{10} \tilde{A}(\alpha)$ values of samples R500−8 and Rfc-8 differ by 0.37 at α = 0.5 (Figure 3b), which means that the corresponding reaction rates differ by a factor of 2.3 at α = 0.5 in this model at any heating program.

4. BIOMASS COMBUSTION

4.1. About the Experiments Reevaluated. Two lignocellulosic samples, a wheat straw sample as an agricultural byproduct and a willow sample from an energy farm were reevaluated from the work of Várhegyi et al.[12] TGA experiments were carried out in gas flows of nitrogen−oxygen mixtures with 4 and 20% (v/v) oxygen. Three linear and two stepwise temperature programs were employed in each case. Figure 4 compares the combustion of the samples at 20 °C/min heating. The combustion of the wheat straw takes place at lower temperatures than that of the willow. This can be due to catalytic effects caused by the higher ash content of the wheat straw.[12] The effect of the oxygen concentration in the ambient gas is also illustrated in Figure 4.

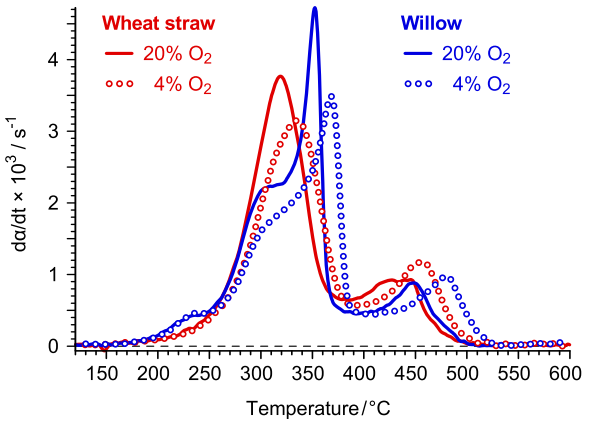

Figure 4. Comparison of the combustion of the biomass samples at 20 °C/min heating in 20% oxygen (solid lines) and in 4% oxygen (circles).

4.2. Least-Squares Evaluation by Approaches I and II. When the data were evaluated by the methods of the present work, first, approach I of the previous section was carried out. Each sample at each oxygen concentration was evaluated separately from the others, hence the method of least squares (eq 10) was based on five experiments in a group. The combustion of lignocellulosic material results in two major peaks in the derivative TGA curves: one for the thermal decomposition and another for the char burn-off. Besides, the pyrolysis of many deciduous trees occurs in two visible partial peaks: one for hemicellulose and another for cellulose. The present model cannot mimic this behavior when the order of the polynomials is less than 7 in eq 8. Accordingly, Table 2 lists the evaluations only from n = 7. When the evaluation was carried out by approach II, identical activation energy was assumed for the two samples at both oxygen concentrations. It is interesting to observe that, practically, the same fit qualities were observed in the two approaches at a given order of polynomial. The fit quality itself improved with n until around n = 11 and was nearly the same at n = 11 and n = 13. The obtained activation energy values, however, did not depend on n; the variation was only 1 kJ/mol within both approaches. In our opinion, all model variants in Table 2 are suitable for practical applications. The ones at n = 11 are illustrated by figures in the same ways as in the previous section: the best, worst, and typical fit qualities were selected from approach I

Table 2. Evaluations of Wheat Straw and Willow Samples with Different Degrees of Polynomials[a,b]

approach	n	reldev$_{20}$	$E_{average}$	E_{lowest}	$E_{highest}$
I	7	4.1	156	148	171
I	8	3.8	156	149	172
I	9	3.4	156	148	172
I	10	3.3	156	148	172
I	11	3.1	156	147	172
I	12	3.1	156	147	172
I	13	3.0	156	147	173
II	7	4.2	154		
II	9	3.5	154		
II	11	3.3	153		
II	13	3.2	153		

[a]In total, 20 experiments on two biomass samples and two oxygen concentrations were evaluated by two approaches employing different degrees of polynomials, n, in the model. reldev$_{20}$ is the root-mean-square relative deviation calculated for the 20 experiments. The lowest and highest E values are not listed for the evaluations by approach II because the E values were identical there. [b]The dimensions of E and reldev$_{20}$ are kJ/mol and %. See the text for further details.

https://dx.doi.org/10.1021/acs.energyfuels.0c03248
Energy Fuels XXXX, XXX, XXX−XXX

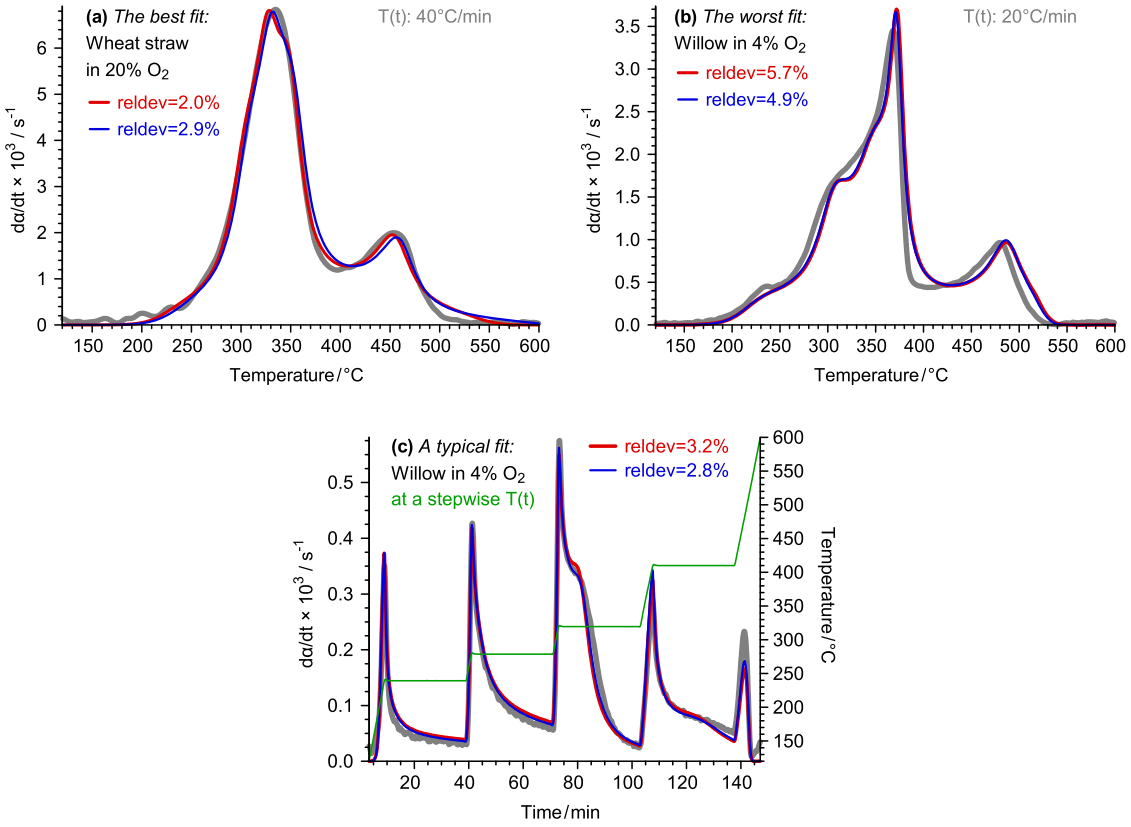

Figure 5. Illustration of the best (a), worst (b), and typical (c) fit qualities obtained for the biomass samples by approach I at n = 11. The corresponding $(d\alpha/dt)^{calc}$ curves are denoted by red color. The $(d\alpha/dt)^{calc}$ curves determined by approach II for the same experiments are shown by thin blue lines. The thick gray lines represent the $(d\alpha/dt)^{obs}$ curves. The thin green line in (c) shows a stepwise temperature program.

for Figure 5. The corresponding $(d\alpha/dt)^{calc}$ curves are denoted by red color for approach I. The curves from approach II for the same experiments were also included in Figure 5; they were represented by thin blue lines. The Supporting Information contains all of the 20 figures from approach II at n = 11.

4.3. Comparing the Reactivities at Identical Activation Energy. When the activation energy is identical for both samples at both oxygen concentrations, the reactivity differences can easily be studied as functions of α, as outlined in Section 3.4. Figure 6 shows this comparison. The wheat straw and willow samples are denoted by red and blue colors, while the higher and lower oxygen concentrations are distinguished by solid curves and circles, respectively. All curves start with a drop between α = 0 and $\alpha \approx 0.1$. It has been known for decades that the first chemical event of the biomass pyrolysis is the thermal decomposition of the thermally labile groups.[38,39] The initial reactivity drop shown in Figure 6 corresponds to these early observations. Figure 6 shows a larger reactivity drop between $\alpha \approx 0.7$ and $\alpha \approx 0.8$. This drop belongs to the termination of the thermal decomposition and the start of the char burn-off (Figure 5a,b). The lower reactivity of the char burn-off is not a surprise because the char burn-off occurs at higher temperatures than the main pyrolysis reactions.

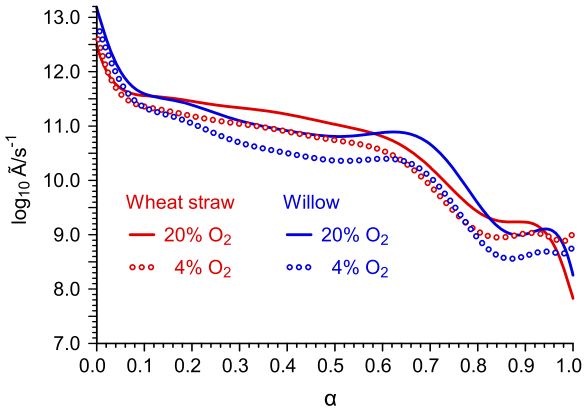

Figure 6. The functions of $\log_{10}\tilde{A}(\alpha)$ for wheat straw (red) and willow (blue) at E = 153 kJ/mol and n = 11.

The comparison of the reactivity at 20 and 4% oxygen (i.e., the comparison of the solid lines to the circles at a given color in Figure 6) gives a graphical picture of the role of the oxygen in the various parts of the reaction. For the wheat straw sample, the difference between the corresponding $\log_{10}\tilde{A}(\alpha)$ curves, $\Delta \log_{10}\tilde{A}(\alpha)$, was 0.1 at α = 0.05 and gradually increased till $\alpha \approx 0.75$, where it had a maximum of 0.36. For the willow sample, $\Delta \log_{10}\tilde{A}(\alpha)$ was 0.2 at α = 0.05 and gradually increased till $\alpha \approx 0.75$, where it had a maximum of 0.67. If the dependence on the oxygen concentration is expressed in a usual way as a power of the oxygen concentration,[1] then the highest oxygen dependences in the present work correspond to reaction orders of 0.5 and 1 for the wheat straw and willow samples, respectively.

5. CONCLUSIONS

(1) An empirical kinetic model from the earlier works of the authors[28,30] was adapted for the combustion of charcoal and biomass samples. Its performance was tested by the

https://dx.doi.org/10.1021/acs.energyfuels.0c03248
Energy Fuels XXXX, XXX, XXX−XXX

reevaluation of 38 TGA experiments from earlier publications. The adjustable parameters of the model were determined by the method of least squares by evaluating groups of experiments together. The procedure aimed at finding best-fitting models for the derivative of the reacted fraction, $(d\alpha/dt)^{obs}$.

(2) In the model variants applied here, a constant E was employed for the whole process. The change of the reactivity during the progress of the reactions was described by the rest of the kinetic equation, eq 2, using suitable approximations for $[A(\alpha)f(\alpha)]$. The approximation was based on polynomials. The degree of polynomials was higher than in the case of biomass pyrolysis in the preceding works of the authors. The gradual increase of the polynomial orders did not change the obtained E values, while the fit quality improved.

(3) Polynomial orders from 5 to 13 gave practically the same E in the evaluation of the 18 charcoal experiments. The samples showed irregular derivative TGA curves, DTG, due to the inhomogeneities forming in the charcoal preparation. Higher polynomial orders helped to describe these irregular shapes.

(4) The DTG curves of the lignocellulosic materials usually exhibit two or three partial peaks during combustion. Polynomial orders from 7 to 13 were used in their modeling. The different polynomial orders resulted in practically identical E values.

(5) It was possible to describe different samples by identical E values. The fit quality only slightly worsened so. This procedure allows an easy comparison of the reactivities of the different samples as a function of the reacted fraction. When a given sample is evaluated with the same E value at different oxygen concentrations, the effect of the oxygen concentration can be surveyed as a function of the reacted fraction.

■ ASSOCIATED CONTENT

Supporting Information

The Supporting Information is available free of charge at https://pubs.acs.org/doi/10.1021/acs.energyfuels.0c03248.

Obtained parameters are presented together with figures of the fit quality for 38 experiments evaluated by approach II and a brief computer code is also given for the calculations with the models presented (PDF)

■ AUTHOR INFORMATION

Corresponding Author

Gábor Várhegyi − *Institute of Materials and Environmental Chemistry, Research Centre for Natural Sciences, Budapest 1519, Hungary;* orcid.org/0000-0002-2933-1845; Phone: +36 12461894; Email: varhegyi.gabor@ttk.mta.hu

Authors

Liang Wang − *SINTEF Energy Research, NO-7465 Trondheim, Norway;* orcid.org/0000-0002-1458-7653

Øyvind Skreiberg − *SINTEF Energy Research, NO-7465 Trondheim, Norway*

Complete contact information is available at: https://pubs.acs.org/10.1021/acs.energyfuels.0c03248

Notes

The authors declare no competing financial interest.

■ ACKNOWLEDGMENTS

The authors acknowledge the financial support by the Research Council of Norway and several industrial partners through the project BioCarbUp ("Optimizing the biocarbon value chain for sustainable metallurgical industry", Project Number 294679/E20). Besides, we are grateful to our co-authors in the earlier works that provided the TGA experiments for the present reevaluations:[12,16] Michael J. Antal, Zsuzsanna Czégény, Morten Grønli, Sándor Könczöl, Ferencz Lezsovits, Tian Li, and Zoltán Sebestyén.

■ NOMENCLATURE

α = reacted fraction (dimensionless)
$A(\alpha)$ = pre-exponential factor (s^{-1})
$\tilde{A}(\alpha) = A(\alpha)f(\alpha)/(1-\alpha)$ at $\alpha < 1$ (s^{-1})
b, c = coefficients in the polynomial approximations of $\ln \tilde{A}(\alpha)$ in eqs 6 and 8 ($\ln s^{-1}$)
E = activation energy [kJ/mol]
$f(\alpha)$ = function in eqs 1 and 2 (dimensionless)
$g(\alpha)$ = the integral of $1/[A(\alpha)f(\alpha)]$ in eq 3 (dimensionless)
h_j = height of an experimental $d\alpha/dt$ curve (s^{-1})
m = the mass of the sample normalized by the initial dry sample mass (dimensionless)
of = objective function minimized by the method of least squares (dimensionless)
n = the order of polynomials in the approximation of $\ln \tilde{A}(\alpha)$
N_{exper} = number of the experiments evaluated together by the method of least squares
N_j = number of the evaluated data on the jth experimental curve
R = gas constant (8.3143×10^{-3} kJ mol^{-1} K^{-1})
reldev = the deviation between the observed and calculated data expressed as a percent of the corresponding peak height (%)
$reldev_{18}$ and $reldev_{20}$ = root mean square of the reldev values of 18 and 20 experiments, respectively (%)
t = time (s)
T = temperature (°C, K)
$T_1(x)$ ... $T_{13}(x)$ = Chebyshev polynomials of the first kind
$x = 2\alpha - 1$ (dimensionless)

■ SUBSCRIPTS

i = digitized point on an experimental curve
j = experiment

■ REFERENCES

(1) Di Blasi, C. Combustion and gasification rates of lignocellulosic chars. *Prog. Energy Combust. Sci.* **2009**, *35*, 121−140.

(2) Branca, C.; Di Blasi, C. Self-heating effects in the thermogravimetric analysis of wood char oxidation. *Fuel* **2020**, *276*, No. 118012.

(3) Bhatia, S. K.; Perlmutter, D. D. A random pore model for fluid-solid reactions: I. Isothermal kinetic control. *AIChE J.* **1980**, *26*, 379−386.

(4) Gavalas, G. R. A random capillary model with application to char gasification at chemically controlled rates. *AIChE J.* **1980**, *26*, 577−585.

(5) Reyes, S.; Jensen, K. F. Percolation concepts in modeling of gas-solid reactions. I. Application to char gasification in the kinetic regime. *Chem. Eng. Sci.* **1986**, *41*, 333−343.

(6) Branca, C.; Di Blasi, C. Global kinetics of wood char devolatilization and combustion. *Energy Fuels* **2003**, *17*, 1609−1615.

(7) Várhegyi, G.; Mészáros, E.; Antal, M. J., Jr.; Bourke, J.; Jakab, E. Combustion kinetics of corncob charcoal and partially demineralized corncob charcoal in the kinetic regime. *Ind. Eng. Chem. Res.* **2006**, *45*, 4962−4970.
(8) Branca, C.; Iannace, A.; Di Blasi, C. Devolatilization and Combustion Kinetics of Quercus cerris Bark. *Energy Fuels* **2007**, *21*, 1078−84.
(9) Várhegyi, G.; Czégény, Zs.; Liu, C.; McAdam, K. Thermogravimetric analysis of tobacco combustion assuming DAEM devolatilization and empirical char-burnoff kinetics. *Ind. Eng. Chem. Res.* **2010**, *49*, 1591−1599.
(10) Anca-Couce, A.; Zobel, N.; Berger, A.; Behrendt, F. Smouldering of pine wood: Kinetics and reaction heats. *Combustion Flame* **2012**, *159*, 1708−1719.
(11) Broström, M.; Nordin, A.; Pommer, L.; Branca, C.; Di Blasi, C. Influence of torrefaction on the devolatilization and oxidation kinetics of wood. *J. Anal. Appl. Pyrolysis* **2012**, *96*, 100−109.
(12) Várhegyi, G.; Sebestyén, Z.; Czégény, Z.; Lezsovits, F.; Könczöl, S. Combustion kinetics of biomass materials in the kinetic regime. *Energy Fuels* **2012**, *26*, 1323−1335.
(13) Tapasvi, D.; Khalil, R.; Várhegyi, G.; Skreiberg, Ø.; Tran, K.-Q.; Grønli, M. Kinetic behavior of torrefied biomass in an oxidative environment. *Energy Fuels* **2013**, *27*, 1050−1060.
(14) Branca, C.; Di Blasi, C. Char structure and combustion kinetics of a phenolic-impregnated honeycomb material. *Ind. Eng. Chem. Res.* **2013**, *52*, 14574−14582.
(15) Branca, C.; Di Blasi, C. Thermogravimetric analysis of the combustion of dry distiller's grains with solubles (DDGS) and pyrolysis char under kinetic control. *Fuel Process. Technol.* **2015**, *129*, 67−74.
(16) Wang, L.; Várhegyi, G.; Skreiberg, Ø.; Li, T.; Grønli, M.; Antal, M. J. Combustion characteristics of biomass charcoals produced at different carbonization conditions. A kinetic study. *Energy Fuels* **2016**, *30*, 3186−3197.
(17) Szűcs, T.; Szentannai, P.; Szilágyi, I. M.; Bakos, L. P. Comparing different reaction models for combustion kinetics of solid recovered fuel. *J. Therm. Anal. Calorim.* **2020**, *139*, 555−565.
(18) Dong, X.; Guo, S.; Ma, M.; Zheng, H.; Gao, X.; Wang, S.; Zhang, H. Hydrothermal carbonization of millet stalk and dilute-acid-impregnated millet stalk: combustion behaviors of hydrochars by thermogravimetric analysis and a novel mixed-function fitting method. *Fuel* **2020**, *273*, No. 117734.
(19) López, R.; Fernández, C.; Cara, J.; Martínez, O.; Sánchez, M. E. Differences between combustion and oxy-combustion of corn and corn−rape blend using thermogravimetric analysis. *Fuel Process. Technol.* **2014**, *128*, 376−387.
(20) Wu, W.; Mei, Y.; Zhang, L.; Liu, R.; Cai, J. Kinetics and reaction chemistry of pyrolysis and combustion of tobacco waste. *Fuel* **2015**, *156*, 71−80.
(21) Yu, Y.; Fu, X.; Yu, L.; Liu, R.; Cai, J. Combustion kinetics of pine sawdust biochar. *J. Therm. Anal. Calorim.* **2016**, *124*, 1641−1649.
(22) Álvarez, A.; Pizarro, C.; García, R.; Bueno, J. L.; Lavín, A. G. Determination of kinetic parameters for biomass combustion. *Bioresour. Technol.* **2016**, *216*, 36−43.
(23) Lotfi, S.; Mollaabbasi, R.; Patience, G. S. Kinetics of softwood kraft lignin inert and oxidative thermolysis. *Biomass Bioenergy* **2018**, *109*, 239−248.
(24) Barzegar, R.; Yozgatligil, A.; Olgun, H.; Atimtay, A. T. TGA and kinetic study of different torrefaction conditions of wood biomass under air and oxy-fuel combustion atmospheres. *J. Energy Inst.* **2020**, *93*, 889−898.
(25) Laougé, Z. B.; Merdun, H. Pyrolysis and combustion kinetics of Sida cordifolia L. using thermogravimetric analysis. *Biores. Technol.* **2020**, *299*, No. 122602.
(26) Xu, X.; Pan, R.; Chen, R.; Zhang, D. Comparative Pyrolysis Characteristics and Kinetics of Typical Hardwood in Inert and Oxygenous Atmosphere. *Appl. Biochem. Biotechnol.* **2020**, *190*, 90−112.
(27) Vyazovkin, S.; Burnham, A. K.; Criado, J. M.; Pérez-Maqueda, L. A.; Popescu, C.; Sbirrazzuoli, N. ICTAC Kinetics Committee recommendations for performing kinetic computations on thermal analysis data. *Thermochim. Acta* **2011**, *520*, 1−19.
(28) Várhegyi, G. Empirical models with constant and variable activation energy for biomass pyrolysis. *Energy Fuels* **2019**, *33*, 2348−2358.
(29) Compendium of Chemical Terminology, *Gold Book*, version 2.3.3; International Union of Pureand Applied Chemistry. https://goldbook.iupac.org/pdf/goldbook.pdf, 2014.
(30) Várhegyi, G.; Wang, L.; Skreiberg, Ø. Non-isothermal kinetics: best-fitting empirical models instead of model-free methods. *J. Therm. Anal. Calorim.* **2020**, *142*, 1043−1054.
(31) De Boor, C. A Practical Guide to Splines. In *Applied Mathematical Sciences*, revised Edition; Springer: New York, 2001; Vol. *27*.
(32) Várhegyi, G.; Chen, H.; Godoy, S. Thermal decomposition of wheat, oat, barley and *Brassica carinata* straws. A kinetic study. *Energy Fuels* **2009**, *23*, 646−652.
(33) Press, W. H.; Flannery, B. P.; Teukolsky, S. A.; Vetterling, W. T. *Numerical Recipes. The Art of Scientific Computing*, 2nd ed.; Cambridge University Press: Cambridge (U.K.), 1992.
(34) Kolda, T. G.; Lewis, R. M.; Torczon, V. Optimization by direct search: New perspectives on some classical and modern methods. *SIAM Rev.* **2003**, *45*, 385−482.
(35) Grønli, M.; Antal, M. J., Jr.; Várhegyi, G. A round-robin study of cellulose pyrolysis kinetics by thermogravimetry. *Ind. Eng. Chem. Res.* **1999**, *38*, 2238−2244.
(36) Radović, L. R.; Walker, P. L., Jr.; Jenkins, R. G. Importance of carbon active sites in the gasification of coal chars. *Fuel* **1983**, *62*, 849−856.
(37) Kyotani, T.; Leon y Leon, C. A.; Radović, L. R. Simulation of carbon gasification kinetics using an edge recession model. *AIChE J.* **1993**, *39*, 1178−1185.
(38) DeGroot, W. F.; Pan, W.-P.; Rahman, M. D.; Richards, G. N. First chemical events in pyrolysis of wood. *J. Anal. Appl. Pyrolysis* **1988**, *13*, 221−231.
(39) Várhegyi, G.; Jakab, E.; Till, F.; Székely, T. Thermogravimetric - mass spectrometric characterization of the thermal decomposition of sunflower stem. *Energy Fuels* **1989**, *3*, 755−760.

https://dx.doi.org/10.1021/acs.energyfuels.0c03248
Energy Fuels XXXX, XXX, XXX−XXX